Analytica Chimica Acta 1316 (2024) 342811

Contents lists available at ScienceDirect

Analytica Chimica Acta

journal homepage: www.elsevier.com/locate/aca

Ammonium bicarbonate buffers combined with hybrid surface technology columns improve the peak shape of strongly tailing lipids

Jenny M. Nilsson [a], David Balgoma [a,b], Curt Pettersson [a], Hans Lennernäs [c], Femke Heindryckx [d], Mikael Hedeland [a,*]

[a] Department of Medicinal Chemistry, Uppsala Biomedical Centre, Uppsala University, Box 574, 75123 Uppsala, Sweden
[b] Instituto de Biomedicina y Genética Molecular (IBGM), CSIC-Universidad de Valladolid, C/ Sanz y Forés 3, 47003, Valladolid, Spain
[c] Department of Pharmaceutical Biosciences, Uppsala Biomedical Centre, Uppsala University, Box 591, 75123 Uppsala, Sweden
[d] Department of Medical Cell Biology, Uppsala Biomedical Centre, Uppsala University, Box 571, 75123 Uppsala, Sweden

HIGHLIGHTS

- Reduced peak tailing of chromatographically problematic lipids.
- Ammonium bicarbonate (ABC) buffers enabled the detection of cardiolipins in liver.
- Overall increased detectability of the major phospho- and sphingolipids.
- HST-CSH C18 column improved peak shape of PAs compared to BEH C18 column.
- ABC buffer with HST-CSH C18 column provides a wider coverage of the lipidome.

GRAPHICAL ABSTRACT

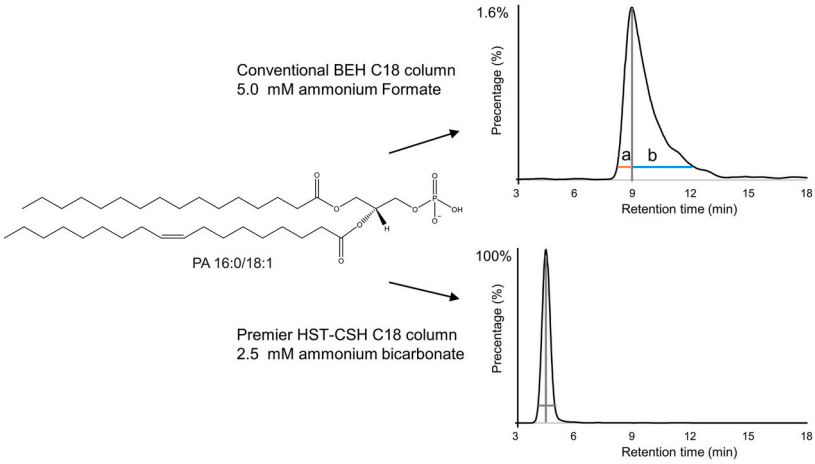

ARTICLE INFO

Keywords:
Phosphatidic acid
Cardiolipins
Lipids
Ammonium bicarbonate
Chromatographic peak shape
Asymmetry factor

ABSTRACT

Background: Lipids such as phosphatidic acids (PAs) and cardiolipins (CLs) present strongly tailing peaks in reversed phase liquid chromatography, which entails low detectability. They are usually analyzed by hydrophilic interaction liquid chromatography (HILIC), which hampers high-throughput lipidomics. Thus, there is a great need for improved analytical methods in order to obtain a broader coverage of the lipidome in a single chromatographic method. We investigated the effect of ammonium bicarbonate (ABC) on peak asymmetry and detectability, in comparison with ammonium formate (AFO) on both a conventional BEH C18 column and an HST-CSH C18 column.

Results: The combination of 2.5 mM ABC buffer pH 8 with an HST-CSH C18 column produced significantly improved results, reducing the asymmetry factor at 10 % peak height of PA 16:0/18:1 from 8.4 to 1.6.

* Corresponding author
E-mail address: mikael.hedeland@ilk.uu.se (M. Hedeland).

https://doi.org/10.1016/j.aca.2024.342811
Received 4 April 2024; Received in revised form 30 May 2024; Accepted 31 May 2024
Available online 8 June 2024

Furthermore, on average, there was up to a 54-fold enhancement in the peak height of its $[M-H]^-$ ion compared to AFO and the BEH C18 column. We confirmed this beneficial effect on other strongly tailing lipids, with accessible phosphate moieties e.g., cardiolipins, phosphatidylinositol phosphate, phosphatidylinositol bisphosphate, phosphorylated ceramide and phosphorylated sphingosine. Furthermore, we found an increased detectability of phospho- and sphingolipids up to 28 times in negative mode when using an HST-CSH C18 column. The method was successfully applied to mouse liver samples, where previously undetected endogenous phospholipids could be analyzed with improved chromatographic separation.

Significance: In conclusion, the use of 2.5 mM ABC substantially improved the peak shape of PAs and enhanced the detectability of the lipidome in negative mode on an RPLC-ESI-Q-TOF-MS system on both BEH C18 and HST-CSH C18 columns. This method provides a wider coverage of the lipidome with one single injection for future lipidomic applications in negative mode.

1. Introduction

Phospholipids (PLs) play a key role in multiple cellular functions, including the formation and fluidity of cell membranes. PLs exist as a mixture of different lipid classes that differ in their polar head group and are present in a wide range of concentrations, which increases the demands of broad analytical methods [1–3]. Specifically, phosphatidic acid (PA) is a relatively simple and low abundant PL that presents a phosphate group in the *sn*-3 position of the glycerol as polar head group [2,4,5]. Accurate analysis of PAs is fundamental in lipidomics, because they act as lipid mediators, secondary messengers and are intermediates in the metabolism of more complex lipids such as triacylglycerols (TGs) and phosphatidylcholines (PCs) [6–8]. However, PAs, cardiolipins (CLs), phosphatidylserines (PSs) and their lyso forms (LPAs, LCLs, and LPSs) give broad and tailing peaks in reversed-phase (RP) liquid chromatography [9–12]. Thus, their analysis constitutes a bottleneck in the deployment of high-throughput lipidomics.

These strongly tailing lipids have accessible phosphoric or carboxylic moieties, (phosphates or an esterified serine) that may form secondary interactions to the stationary phase, which decrease their detectability [9–12]. Peak tailing is believed to arise from two types of secondary interactions: (i) active metal ion complexing, between ions from the LC-flow path and the accessible phosphate or serine moieties [10,13–16] and/or (ii) silanophilic interactions, which are highly dependent on pH [13,15].

Traditionally, to reduce these secondary interactions, different additives such as phosphoric acid [9,17,18] and EDTA [12,19] have been used to minimize this metal-phosphate interaction when analyzing PAs. However, over time, these non-volatile additives risk a decreased sensitivity in ESI-MS due ion suppression and risk of clogging of the ion source and even permanently damaging the mass spectrometer in the case of phosphoric acid.

Recently, the hybrid surface technology (HST® Waters Corporation) has been developed [20–22]. HST uses an ethylene-bridge siloxane polymer to provide a barrier between the analytes and metal surfaces of the solid support as well as in the flow path [10,20]. In a lipidomics application, Isaac et al. [10] used an HST-CSH C18 column with an ammonium formate (AFO) buffer. They found that the HST chromatographic system (chromatograph and column) reduced the peak tailing and increased the detectability for PAs, PSs, LPAs and LPSs. Unfortunately, HST chromatographic systems are not generally available and the beneficial effect of HST columns in traditional chromatographs is not fully known.

Complementarily, Asakawa et al. [15] have shown that ammonium bicarbonate (ABC) buffers reduce peak tailing of nucleotide phosphate compounds on a Capcellpak C18-AQ column. They suggested that ABC reduces the secondary interactions of phosphorylated compounds by both complexing metal ions and decreasing silanophilic interaction at pH above 5. Gertner et al. [23] recently showed that the use of ABC buffers increases the detectability and chromatographic behavior of phosphatidylinositide species, including oxidized and phosphorylated species. Additionally, in the heated gas-phase of ESI chambers, it has been described that ABC degrades readily to carbon dioxide, ammonia and water, which improves deprotonation and enhances ionization in negative mode [24]. Regarding the structural determination of lipids from this adduct, the initial studies did not elucidate the fragmentation patterns of the adduct $[M+HCO_3]^-$ of lipids with choline moieties [25]. Nevertheless, Zhao et al. have recently elucidated the structure of PCs, lysophosphatidylcholines (LPCs) and sphingomyelins (SMs) from the fragmentation of the adduct $[M+HCO_3]^-$ [26–28]. Despite these advances, it is not known if ABC reduces the peak asymmetry of strongly tailing lipids and improves the detectability of the lipidome.

In this context, we hypothesized that the combination of ABC buffers and HST columns would improve the coverage of the lipidome by RPLC on conventional chromatographs. To investigate this hypothesis, we compared AFO and ABC as mobile phase buffers on both a BEH C18 column and an HST-CSH C18 column. Subsequently, we evaluated the peak asymmetry and detectability of the lipidome, focusing on PAs as a paradigmatic lipid among the strongly tailing lipids. Our results strongly suggest that the combination of ABC buffers with HST CSH C18 columns allows a broader coverage of the lipidome on traditional chromatographs with a single RPLC injection, enhancing high-throughput lipidomics.

2. Materials and methods

2.1. Chemicals

Egg chicken PA cat# 840101 (a mixture of different PAs were the fatty acid distribution 16:0 and 18:1 are the most abundant fatty acyl chains), the internal standard (IS) PG 17:0/17:0, phosphatidylinositol phosphate (PI(3)P-18:1), phosphatidylinositol bisphosphate (PI(4,5)P-18:1) phosphorylated ceramide (CerP d18:0/16:0) and phosphorylated sphingosine (S–1P d18:1) were all purchased from Avanti Polar Lipids Inc. (Alabaster, AL, USA).

Acetonitrile (ACN), methanol (MeOH), 2-propanol (IPA) and formic acid (HCOOH) were all of LC-MS grade and were purchased from Fischer Scientific (Loughborough, UK). Ammonium bicarbonate (ABC, NH_4HCO_3) LC-MS grade and chloroform ($CHCl_3$) HPLC grade >99.0 % were purchased from Honeywell (Charlotte, NC, USA). LiChropur® ammonia solution (NH_3) 25 % was LC-MS grade and purchased from Merck (Darmstadt, Germany). Water was deionized and purified by a Milli Q-purification system from Millipore (Bedford, MA, USA).

2.2. Stock solutions and sample preparation

Stock solutions of egg PA were diluted and prepared in MeOH at three concentrations, 0.036 mg mL^{-1}, 0.19 mg mL^{-1} and 0.37 mg mL^{-1}. After sample preparation (section 2.4), the injected concentrations were 0.66 μg mL^{-1}, 3.1 μg mL^{-1} and 6.3 μg mL^{-1}, respectively referred to as, *Low, Middle* and *High*. As IS, 10 μL of a solution of 7.725 mg mL^{-1} PG 17:0/17:0, in ACN/IPA (50:50, v/v) was used. PI(3)P- 18:1, PI(4,5)P-18:1, CerP d18:0/16:0 and S–1P d18:1 were diluted with ACN/IPA/water (3:3:2, v/v/v) to a concentration of 5.0 μg mL^{-1}, 5.0 μg mL^{-1}, 0.5 μg mL^{-1} and 0.5 μg mL^{-1}, respectively.

A stock solution of 200 mM ammonium bicarbonate buffer pH 8.0 to

prepare the mobile phases was prepared with water/MeOH (9:1, v/v), aliquoted and frozen at −20 °C.

2.3. Chromatographic conditions and MS-settings

Different mobile phase buffers were compared and studied: mobile phase A) IPA/ACN/water (15:35:50, v/v/v) and B) IPA/ACN/water (70:25:5, v/v/v) with different buffers in total concentration: (i) 5.0 mM AFO pH 9.0, or (ii) 2.5 mM, 5.0 mM or 10 mM ABC pH 8.1. To avoid potential clogging of the column or get unnecessary particles into the system, we filtered the ammonium bicarbonate before addition to the mobile phase.

An Acquity UHPLC I-Class chromatograph equipped with a Flow Through Needle (FTN) injection system was used for the chromatographic separations. Two types of columns were used: (i) an Acquity Premier™ CSH C18 with a VanGuard™ FIT, 130 Å, 1.7 μm, 2.1 × 100 mm column (referred to as HST-CSH C18 in the rest of the text); and (ii) an Acquity™ UPLC® BEH C18, 130 Å, 1.7 μm, 2.1 × 100 mm column (Waters Corporation, Milford, MA, referred to as BEH C18 in the rest of the text). For both columns, the flow-rate was 0.3 mL min^{-1}, injection volume 1.0 μL and column temperature 55 °C. A linear gradient was used: 0–2.50 min, 20 % B to 45 % B; 2.50–4.0 min, 45 % to 65%B; 4.0–11 min, 65 % B to 85 % B; 11–14 min, 85 % B to 99 % B; 14–20 min, 99 % B, followed by additional washing and equilibration to starting condition with 20 % B for 4 min. The total runtime was 27 min.

The detection was performed by using electrospray ionization (ESI) on a Synapt G2S Q-ToF (Waters) scanning between *m/z* 100 and 1200. The samples were analyzed in negative mode with the capillary voltage at −2.0 kV, cone voltage at −30 V, source and desolvation temperatures were set at 120 °C and 500 °C, respectively. The scan time was set to 1.0 s. Nitrogen was used as desolvation gas with a flow-rate of 800 L h-1 and as cone gas at 10 L h^{-1}. Nebulizer gas flow was always set to 6.0 bar. MS/MS fragmentation was performed using FastDDA with an energy ramp from 10 to 40 V and a scan time of 0.5 s.

Six different conditions were tested for post column infusion: aqueous solution of i) 50 mM ABC pH 8.3, ii) 100 mM ABC pH 8.3, iii) water pH 5.6, iv) formic acidic in water adjusted to pH 3.7, v) ammonia in water adjusted to pH 8.3 with ammonia solution (25 %) and vi) carbonated water made from water carbonated in a SodaStream® at pH 3.8. The flow-rate of post column infusion was 5.0 μL min^{-1}, studied on the HST-CSH column with 5.0 mM AFO as mobile phase buffer and a flow-rate of 0.27 mL min^{-1}.

2.4. Preparation of homogenates and extraction of mouse liver

Approximately 10 mg of mouse liver were mixed with 80 μL of water per mg of liver in Lysing Matrix D tubes (MP Biomedicals, Ohio, USA). Subsequently, the liver was homogenized at 4.0 m s^{-1} for 30 s by using a FastPrep-24 5G homogenizer (MP Biomedicals, Solon, Ohio, USA) [29].

Lipid extraction was performed by a modified Bligh&Dyer method [30]. Briefly, 150 μL of liver homogenate were mixed with $CHCl_3$/MeOH (1:2, v/v) with 1 % of HCOOH. The extraction was repeated and the $CHCl_3$/MeOH phases were mixed and evaporated to dryness before resuspension in 400 μL of ACN/IPA (50:50, v/v). The homogenates were pooled before and after extraction to avoid variability among samples and ensure that the signal intensity variations are due to the LC/MS conditions. In order to assess only the chromatographic variability, the IS and the mix of PA were added after extraction. The blank samples were handled the same, with pooling before and after extraction. The order of the sample preparation and the injection order were randomized. The samples were aliquoted into 9 batches and stored at −80 °C for a minimum of 24 h. A new aliquot of the samples was defrosted and vortexed for every chromatographic condition studied. Quality control samples (QC) were injected every eight injections and consisted of pooled liver extracts with the addition of IS, but no addition of external PA.

The methods were approved by Uppsala ethical committee for animal experimentation (DNR 5.8.18–0089/2020).

2.5. Data analysis

The asymmetry factor was calculated as b/a at 10 % of the peak height (see Graphical Abstract). For this purpose, an R function was developed. Briefly, the script fits the logarithm of the signal with a smoothing spline in order to interpolate the signal to find the full width half maximum (FWHM) and the asymmetry factor at the specified height (between 5 % and 25 % of the peak height). The function is available in ChromAsym, R package at https://github.com/dbalgoma/ChromAsym (see Supplementary Material 3 for its vignette).

Intervals of confidence are expressed as the mean ± the standard deviation to report the variability of our measurements. Finally, rather than on statistically significant results, data analysis and interpretation was focused on effect sizes [31,32]. The signal-to-noise (S/N) ratio were calculated using Masslynx (zero values were ignored). The shorthand lipid nomenclature followed the LIPID MAPS system [33].

3. Results and discussion

Chromatographically problematic lipids, such as PAs, elute as asymmetric and broad peaks in conventional RP-systems, which decreases their detectability (Fig. 1). In our previous studies, PAs and CLs were non-detectable in biological samples using a BEH C18 column with 5.0 mM AFO as aqueous buffer [29,34,35]. To improve their detectability, we modified the mobile phase compositions to A) IPA/ACN/-water (15:35:50) with 5.0 mM of AFO and B) IPA/ACN/water (70:25:5) with 5.0 mM of AFO. This allowed the detection of PA standards at higher concentrations; however, the peaks were still strongly asymmetric (Fig. 1). Subsequently, we pre-washed the chromatographic system with 1.0 M EDTA [9]. This decreased AF_{10} from 10.6 to 6.2 for PA 16:0/18:1, i.e., the peak asymmetry remained to a large degree. In addition, pre-washing the column with EDTA presents several drawbacks: (i) it is time-consuming (>60 min) as it includes column conditioning and chromatograph washing after use and (ii) it increases the risks of clogging of the ESI probe. Consequently, we explored the effect of ABC as aqueous mobile phase buffer in negative mode on strongly tailing lipids, with a special focus on PAs.

3.1. ABC improved peak shape and detectability of PAs on conventional BEH C18 columns

To investigate the effect of ABC buffers on the peak symmetry of strongly tailing lipids on traditional BEH C18 columns, we injected PAs at low and middle concentrations (see section 2.2) (Fig. 1). The ABC buffer strongly decreased the asymmetry of PAs. For example, PA 16:0/18:1 presented a much more symmetric peak when using the ABC buffer instead of the AFO buffer (Fig. 1B and D).

In comparison with the AFO buffer, three factors demonstrated that ABC buffers increased the detectability of PAs: (i) ABC allowed the detection of PA 16:0/18:1 in low concentration, which was not possible with the AFO buffer (Fig. 1A vs Fig. 1C); (ii) ABC increased the peak height of PA 16:0/18:1 at middle concentration by 16.5 ± 1.2 times; and (iii) ABC increased the peak area of PA 16:0/18:1 at middle concentration by 3.7 ± 0.5 times. The increase in area indicates that the improvement in detectability with ABC is not only the result of the improved peak symmetry, but also an increase in the efficiency of ESI in negative mode (see section 3.3 for further investigation).

All together, these observations showed that ABC boosts the detectability of PAs by both a reduction of peak asymmetry and an increase in ESI efficiency (see section 3.3). In order to investigate if the detectability could be improved further, we studied the combined effect of ABC buffers and an HST column.

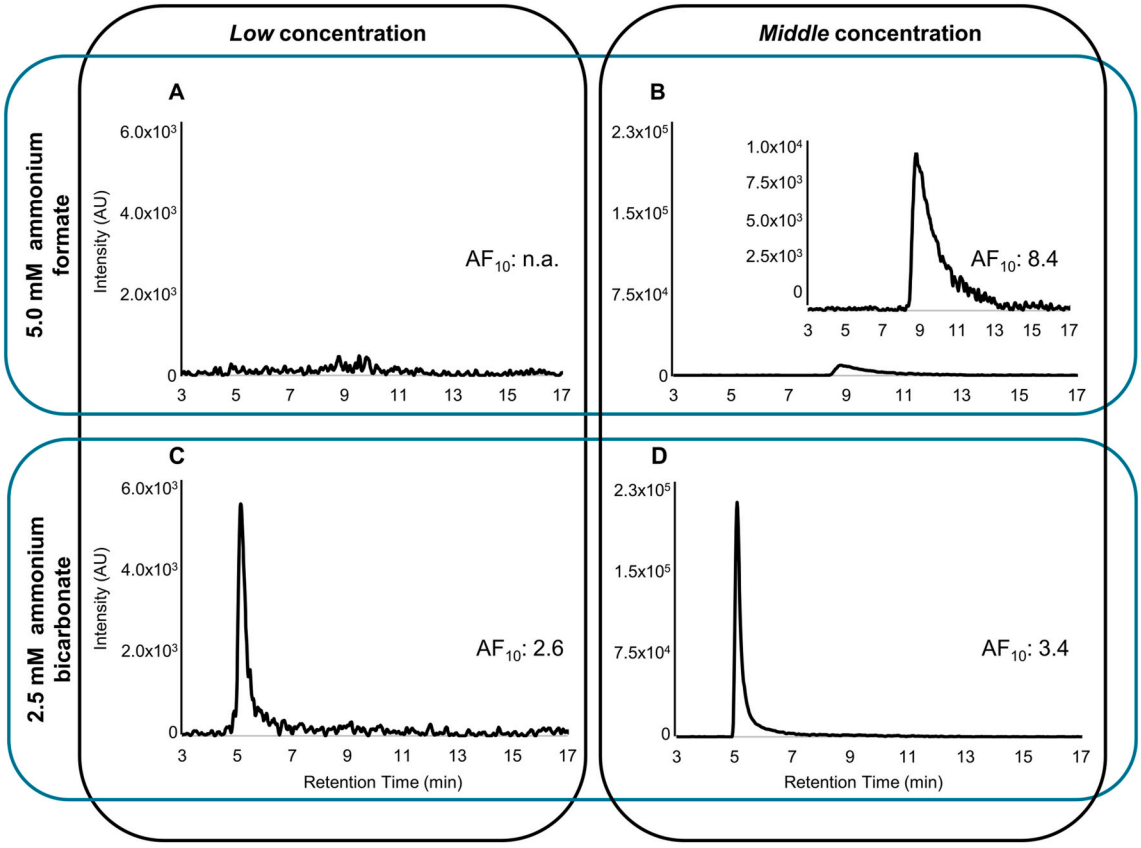

Fig. 1. Effect of buffer type on peak asymmetry. Extracted ion chromatogram of the adduct $[M - H]^-$ of PA 16:0/18: *m/z* 673.4808 ± 15 ppm after separation on a BEH C18 column. (A) Buffer 5.0 mM ammonium formate (AFO) and egg PA injected in Low concentration, the peak was not detectable. (B) Buffer 5.0 mM of AFO and PA injected in middle concentration, the peak was detectable (detail highlighted in a box). (C) Buffer 5.0 mM ammonium bicarbonate (ABC) and egg PA injected in Low concentration. (D) Buffer 5.0 mM ABC and PA injected in middle concentration. n.a. stands for non-applicable; AF_{10} reports the asymmetry factors at 10 % of the peak height. AU denotes Arbitrary Units.

3.2. HST-CSH C18 columns further improved the detectability of strongly tailing lipids

3.2.1. ABC combined with an HST-CSH C18 column strongly improved peak shape and detectability

Considering the results by Isaac et al. [10] about the beneficial use of HST-CSH C18 columns in lipidomics, we investigated the effect of combining a 2.5 mM ABC buffer and an HST-CSH C18 column on the peak symmetry of strongly tailing lipids. As before, we used PA 16:0/18:1 as a model compound.

We made three major observations regarding the performance of the HST-CSH C18 columns and ABC buffers. First, the combination of an HST-CSH C18 column with AFO buffers with pH 9 yielded lower peak asymmetry than the BEH C18 column with the same buffer (Fig. 2). Thus, our results confirm the observations reported by Isaac et al. [10]. Second, the combination of an HST-CSH C18 column and a 2.5 mM ABC buffer pH 8 yielded even lower peak asymmetry (Fig. 2). Third, the combination of HST-CSH C18 column and 2.5 mM ABC buffer strongly increased the peak area and the signal-to-noise ratio (S/N) at different analyte concentrations (Table 1). In summary, the detectability of PA 16:0/18:1 could be greatly improved using a combination of HST-CSH C18 columns and ABC buffers. Based on these results, we investigated the effect on other PAs. While at low concentration, no PAs were detectable with AFO, nine PAs were detectable using a 2.5 mM ABC buffer (Table S1). Furthermore, the detected PAs showed superior peak shape and presented increased detectability using ABC (Table S1). Subsequently, we investigated the behavior of other low abundant phosphorylated lipids of biological interest with accessible phosphate moieties (PIP, PIP2, CerP and S–1P). These lipids also presented an increased detectability and improved peak symmetry when using ABC compared to AFO (Fig. S1).

Collectively, our results indicate that ABC decreases the secondary interactions between the phosphate and serine moieties of strongly tailing lipids and the stationary phase, leading to a general reduction of peak tailing [13,15].

Overall, our results show that the combination of HST-CSH C18 columns and an ABC buffer boosts the detectability of PA and other strongly tailing lipids. Thus, the next step was to investigate the effect on the detectability of strongly tailing lipids of: i) the concentration of ABC in the mobile phases (section 3.2.2); and ii) the concentration of the analytes themselves (section 3.2.3).

3.2.2. Detectability of strongly tailing lipids with different concentrations of ABC buffer

To study the effect of ABC concentration on the peak shape and the detectability of strongly tailing lipids, we compared the chromatographic behavior of PA 16:0/18:1, using three different buffer concentrations (2.5, 5.0 and 10 mM). First, the retention time of PA 16:0/18:1 increased with the concentration of ABC in the mobile phase on both BEH C18 and HST-CSH C18 columns (Fig. 3). This behavior suggests, an ion-pair retention mechanism for the deprotonated PA and ammonium ions, which is expected to increase at higher counter-ion concentrations, or a reduced repulsive electrostatic interaction between negatively charged PA and negatively charged silanol groups.

Second, the peak shape of PA 16:0/18:1 did not change dramatically within the concentration interval 2.5–10 mM of ABC on any of the columns (Fig. 3). This fact indicates that even at 2.5 mM ABC the unspecific interactions are minimized.

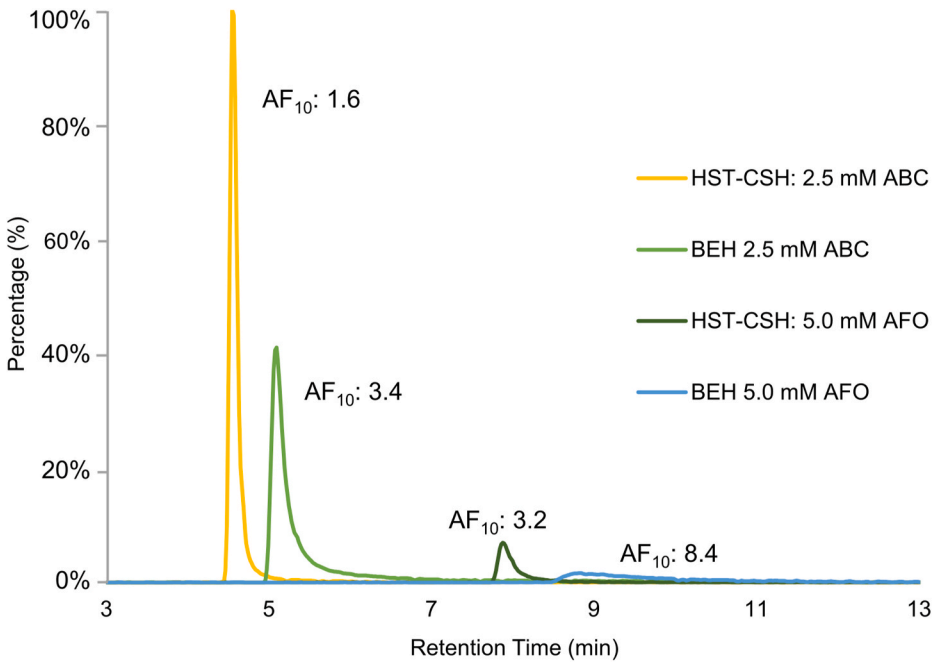

Fig. 2. Effect of column and mobile phase buffer on peak symmetry. The lines represent four extracted ion chromatograms in negative ESI mode of PA 16:0/18:1 with *m/z* 673.4808 ± 15 ppm when using: 1) HST-CSH C18 column with 2.5 mM ammonium bicarbonate (ABC) (yellow); 2) BEH C18 column with 2.5 mM ABC (light green); 3) HST- CSH C18 column with 5.0 mM ammonium formate (AFO) (dark green); and 4) BEH C18 column with 5.0 mM AFO (blue). AF_{10} reports the asymmetry factors at 10 % of the peak height. (For interpretation of the references to color in this figure legend, the reader is referred to the Web version of this article.)

Table 1
Average fold change of peak area, height and signal-to-noise ratio (S/N) of PA 16:0/18:1 between different chromatographic conditions: HST-CSH C18 (CSH) and BEH C18 (BEH) columns combined with 5.0 mM ammonium formate (AFO) and 2.5 mM ammonium bicarbonate (ABC) buffers.

Condition	Low			Middle			High			Average fold change		
	area	height	S/N	area	height	S/N	area	height	S/N	area	height	S/N
CSH_{ABC}/BEH_{AFO}	a	a	a	5.8	63.5	276.4	4.5	44.9	159.7	5.1	54.2	218.0
CSH_{ABC}/CSH_{AFO}	9.7	12.7	14.5	7.0	15.0	33.8	4.7	9.4	21.2	7.1	12.4	23.2
BEH_{ABC}/BEH_{AFO}	a	a	a	4.9	24.9	33.1	4.2	20.2	32.0	4.6	22.6	32.6
CSH_{AFO}/BEH_{AFO}	a	a	a	0.8	4.2	8.2	1.0	4.8	7.6	0.9	4.5	7.9
CSH_{ABC}/BEH_{ABC}	1.1	2.5	2.3	1.2	2.6	8.4	1.1	2.2	5.0	1.1	2.4	5.2

[a] No detectable peak with BEH C18 column and AFO buffer.

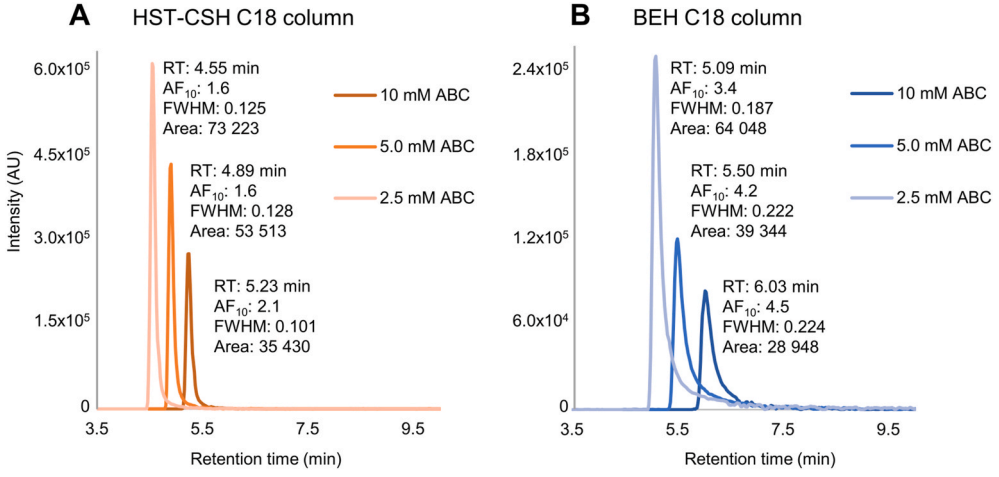

Fig. 3. Effect of ABC concentration on peak symmetry and retention. Extracted ion chromatograms of *m/z* 673.4808 ± 15 ppm from a standard mixture of egg PA when using: (A) an HST-CSH C18 column with 2.5; 5.0 and 10 mM bicarbonate as mobile phase buffer; and (B) a BEH C18 column with 2.5; 5.0 and 10 mM bicarbonate as mobile phase buffer. AU denotes Arbitrary Units.

Third, we found that the higher concentration of ABC, the lower the peak height and area of PA 16:0/18:1 on both columns (Fig. 3). This might be explained by: (i) a higher ion suppression in the ESI chamber with higher salt concentrations and (ii) a lower ionization due to the lower water content in the mobile phase gradient at the increased elution time (Fig. 3).

Finally, the same behavior regarding retention time and detectability was also observed for other strongly tailing lipids, such as PSs and CLs (data not shown).

On the one hand, ABC concentrations higher than 10 mM might be beneficial for decreasing peak asymmetry. However, the decrease in detectability in Fig. 3, suggests that the ionization efficiency would likely decrease. On the other hand, ABC concentrations lower than 2.5 mM might further improve the detectability of the lipids. However, the buffer capacity would be too low, compromising the chromatographic performance. Considering our results and these two opposite factors, the recommended concentration of ABC for improved chromatography and detectability is 2.5 mM.

3.2.3. *The analyte concentration did not affect peak asymmetry on the HST-CSH C18 column*

To evaluate if the peak shape of PA 16:0/18:1 depends on its injected concentration, three levels were spiked into mouse liver extracts at low, middle and high concentrations (see section 2.2 for details). Subsequently, the spiked liver samples were injected on BEH C18 and HST-CSH C18 columns using AFO and ABC as buffers.

On the HST-CSH C18 column, we did not find a pronounced difference in AF_{10} among the three investigated concentrations of PA (Fig. 4A). This suggests that the secondary interactions on the column are minimal and/or the ratio of molecules interacting between the primary and the secondary mechanisms is independent of the concentration of the analyte. Therefore, independently of PA concentration, most of the PA molecules are likely to undergo primary interactions with the HST-CSH C18 column, yielding an overall better peak shape.

In contrast, on the BEH C18 column with ABC buffers, we found that at higher concentrations of spiked PA a reduction by 30 % in AF_{10} was observed (Fig. 4B). We speculate that, at high concentration of PAs on the BEH C18 column, the secondary sites of interaction might be saturated by the analyte. Hence, the ratio of PAs that interact by primary interactions increase, which decreases peak asymmetry. The retention times are unaffected by the analyte concentration, which entails that we are still in the linear range.

On the contrary, when using AFO, the peak asymmetry increased with higher concentrations of PAs on both columns. This suggests that AFO does not lower the ratio of secondary interactions as efficiently as ABC buffers.

To evaluate if AF_{10} had any correlation with the number of carbons (NC) and the number of unsaturations (NU) for PAs, both bubble plots (Fig. S2) and a regression analysis (SM4) was performed. The regression analysis in SM4 showed that ABC 2.5 mM reduced AF_{10} by 1.22 units on the HST-CSH C18 column. No relevant statistical effect on AF_{10} could be detected for the number of acyl carbons, the number of unsaturations, and the peak area.

In summary, when an HST-CSH C18 column was combined with ABC buffers, the peak shape of PA in liver samples did not depend on the concentration of the analytes in the concentration range tested. This indicates an improved chromatographic performance on the HST-CSH C18 column with ABC buffers compared with the BEH C18 column.

3.3. *ABC infused post-column enhanced the efficiency of ionization*

As presented in section 3.2, when using ABC, we observed an increase in both peak height, as well as peak area indicating an increased ionization efficiency. Two factors may explain this behavior. First, as previously suggested by Huang et al. [36], ABC decomposes into CO_2 and H_2O during ESI, forming microbubbles of CO_2 within the electrospray microdroplets. These microbubbles increase the surface area of the liquid-gas interface and thereby improve ionization [36–38]. Second, ABC decreases the retention of the PAs, when compared with AFO, giving rise to a higher percentage of water at the elution time – a factor that could result in an improved ESI efficiency. To elucidate the contribution of these two factors, we studied the ionization efficiency of PAs by post-column infusion of water with and without ABC when AFO buffer was used in the mobile phase with a flow-rate of 0.27 mL min^{-1}.

The post-column infusion of water with a flow-rate 5.0 μL min^{-1} yielded a small dilution effect on the peak height and peak area of PA 16:0/18:1 when compared with no post column infusion (Fig. 5). This suggests that the amount of water from the eluent was not responsible for the enhanced ionization of PA 16:0/18:1.

In contrast, the post-column infusion of 50 mM ABC enhanced the

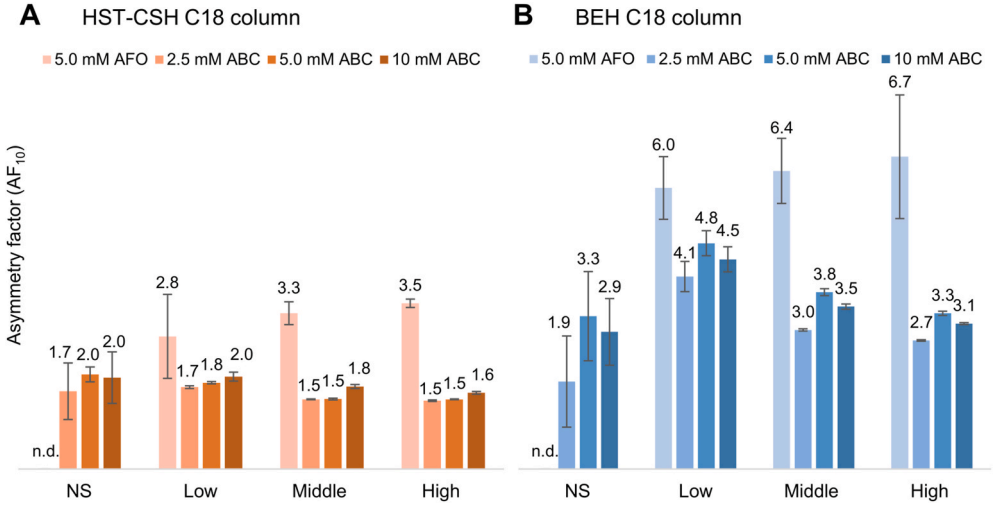

Fig. 4. Comparison of the asymmetry factor among columns, mobile phase buffers, concentration of ammonium bicarbonate and concentration of phosphatidic acid. The peak asymmetry of PA 16:0/18:1 in liver was measured by AF10 values with buffers 5.0 mM ammonium formate (AFO) and 2.5, 5.0 and 10 mM ammonium bicarbonate (ABC). The measurements were done on (A) an HST-CSH C18 columns; and (B) a BEH C18 column. In every chromatographic condition, the bars are showed by the endogenous PA in non-spiked liver matrix (NS, light color) and spiked liver matrix in low, middle and high spiked concentrations (darker colors). Error bars illustrate the variability by the standard deviation (st.dev) for AF_{10} (triplicate injections). (For interpretation of the references to color in this figure legend, the reader is referred to the Web version of this article.)

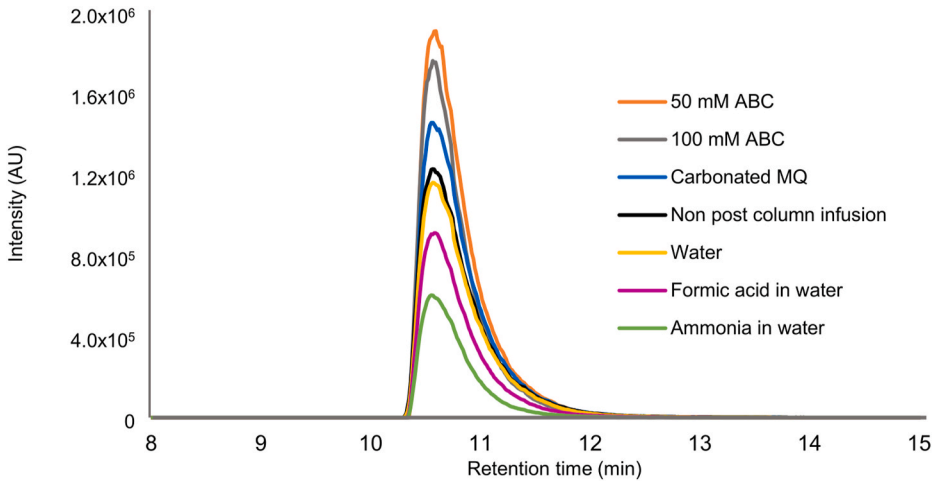

Fig. 5. Effect of CO_2 in electrospray on the detectability of PA 16:0/18:1 in negative ESI. Extracted ion chromatogram of PA 16:0/18:1 $[M-H]^-$ from Egg PA, *m/z* 673.4808 ± 15 ppm. The lipids were separated on an HST-CSH C18 column, using 5.0 mM AFO buffer. The flow rate of post-column infusion was 5.0 μL min^{-1}. AU denotes Arbitrary Units.

intensity of PA 16:0/18:1 1.6-fold (Fig. 5). Nevertheless, the signal decreased slightly with a higher concentration of ABC, possibly due to increased ion suppression.

Interestingly, when compared with pure water, carbonated water enhanced the intensity 1.3-fold of PA 16:0/18:1. Carbonated water had a pH of 3.77 so we wanted to exclude that this effect could be caused by a shift in pH. Consequently, formic acid in water (pH 3.70) and ammonia in water (pH 8.26) were infused. In comparison with the post-column infusion of water, both acidic and basic conditions resulted in a decreased ionization efficiency (0.2-fold and 0.48-fold, respectively). This fact suggests that the pH change was not responsible for the enhanced ionization by the carbonated water (Fig. 5).

Finally, we observed the same behavior for other PAs when pure water, carbonated water, ABC, formic acid and ammonia in water were infused post-column (data not shown).

Taken together, these results suggest that neither the water content nor the pH change enhance the ionization of PAs. Consequently, our experiments strongly suggest that it is the presence of carbonate –and possibly the formation of microbubbles of CO_2 in the microdroplets– enhances the ESI of PAs [24,36–38].

3.4. ABC improves the detectability of the lipidome in biological samples

To evaluate the effect of ABC on biological samples with a complex matrix, mouse liver homogenate was used. As before, we first focused on PAs, using PA16:0/18:1 as a strongly tailing lipid. Subsequently, we evaluated the effect of ABC on the detectability of other lipids in the liver lipidome.

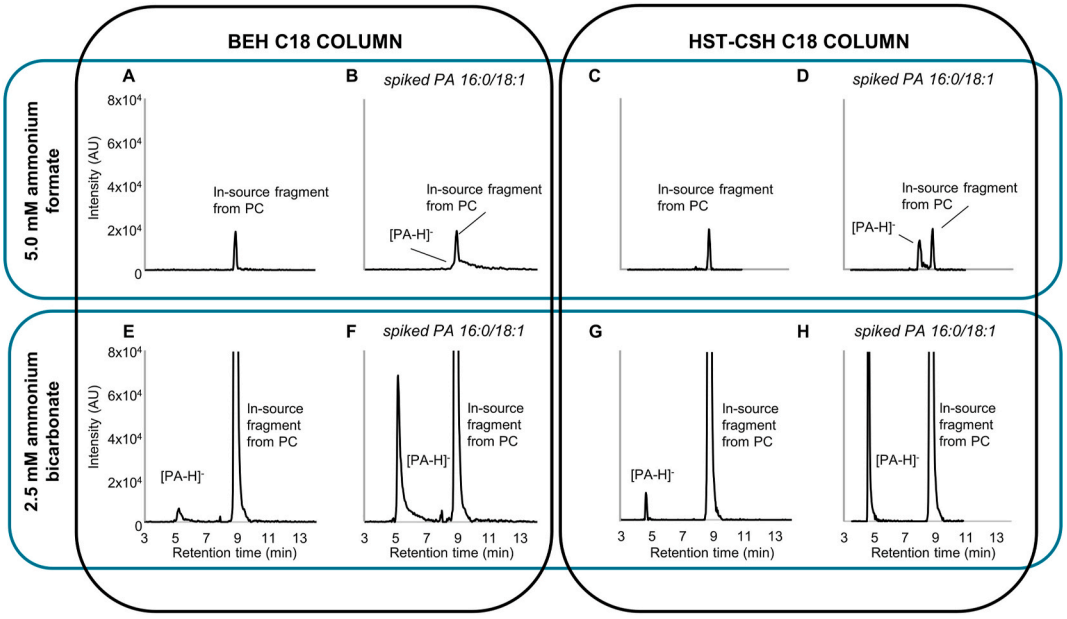

Fig. 6. Effect of buffer, column, and concentration on the detectability of PA 16:0/18:1 in liver samples. We injected non-spiked (panels A, C, E, and G) and low spiked samples in low concentration (panels B, D, F, and H) in combinations of: (i) 5.0 mM ammonium formate buffer and BEH C18 column (panels A and B); (ii) 5.0 mM ammonium formate and HST-CSH C18 column (panels C and D); (iii) 2.5 mM ammonium bicarbonate and BEH C18 column (panels E and F); and (iv) 2.5 mM ammonium bicarbonate and HST-CSH C18 column (panels G and H). Subsequently, *m/z* 673.4808 ± 10 ppm was extracted to detect the adduct $[M-H]^-$ of PA 16:0/18:1. In all cases, an in-source fragment of different adducts of PC 16:0/18:1 was observed, not corresponding to natural occurring PA 16:0/18:1 (denoted as *in-source fragment from PC* in the panels). All panels present the same scale for the X- and the Y-axis. AU denotes Arbitrary Units.

3.4.1. ABC enabled the detection of PA in liver samples

First, we found that endogenous PA 16:0/18:1 was undetectable in liver using AFO as mobile phase buffer (Fig. 6A–C), but could be clearly detected in the presence of ABC buffer on both columns (Fig. 6E–G). In contrast, with the AFO buffer (Fig. 6A–D), PA 16:0/18:1 was only detectable when spiked to the liver homogenate, and analyzed on an HST-CSH C18 column (Fig. 6D). Second, when AFO buffers with the BEH C18 column were combined, we observed that PA 16:0/18:1 coeluted with an isobaric in-source degradation product of PC 16:0/18:1 (Fig. 6B). However, ABC selectively decreased the retention of PAs (from 9.0 to 5.1 min for PA 16:0/18:1), allowing its separate detection in non-spiked and spiked samples (Fig. 6E–H). A slight drift in retention time was observed when using ABC. This drift has so far not been an issue. For example, it only corresponds to 0.46 %RSD for the IS, over 5.5 h of runtime and 13 injections. This drift in retention time is common in lipidomics applications using AFO or ABC. In any case, when processing the data with multivariate methods, QC samples correct for the instrumental drift. Furthermore, we can see that the drift in retention is less pronounced at lower concentrations of ABC. A small intensity drop over the batch can also be observed when we use the ABC buffer. However, we could still detect the lipids with more than a 11-fold higher signal-to-noise ratio with ABC compared to AFO after 21 injections of liver samples.

Remarkably, this increased separation between PAs and other major phospholipids (mainly PCs and PEs, Table S3) reduced the risk of: (i) ion suppression, and (ii) interferences by in-source fragmentations (as in Fig. 6). Consequently, a 2.5 mM ABC buffer also improves the sensitivity and detectability of PAs in biologically complex matrices by increasing its chromatographic resolution from major phospholipids.

3.4.2. ABC enhances the detectability of the lipidome in liver samples

To assess the effect of ABC buffers on the lipidome in a biological sample, we evaluated the detectability of different lipid classes. Because of the advantages of using an HST-CSH C18 column that have been presented, we focused on the effect of 2.5 mM ABC buffer compared with 5.0 mM AFO when using an HST-CSH C18 column. Overall, there was an increase in the detectability of PLs and sphingolipids when using ABC buffers (Fig. 7).

First, considering our results about PAs, we focused on other phospholipids that are chromatographically problematic with traditional separations in lipidomics (C18 chromatography with AFO buffers). We found that 2.5 mM ABC buffer enhanced the detectability of LPAs, LPSs, CLs and PSs through increased peak symmetry, height and area (Table S3). For example, LPS 18:0 and PS 38:4 presented a 1.9- and 4.2-fold increase in peak height, respectively, using ABC (Table S3). Remarkably, with S/N above 3 as criteria for detection, cardiolipins such as CL 72:8 (Fig. 7), CL 72:7, CL 72:6, CL 74:9, CL 74:10 and CL 70:6 were only detectable in the liver samples using 2.5 mM ABC [$[M - 2H]^{2-}$], (Table S3). To increase the coverage of the lipidome, these lipids have been traditionally analyzed in separate runs by using normal phase liquid chromatography (NPLC) [39] or HILIC [40–43] hampering lipidomics throughput. Consequently, the combination of HST-CSH C18 columns with ABC buffers is of special interest for high-throughput lipidomics.

Second, we focused on other major phospholipids and sphingolipids, such as phosphatidylinositol (PIs), PEs, phosphatidylglycerol (PGs), PCs, sphingomyelins (SMs), ceramides (Cer) and hexosylceramide (HexCer) in liver extracts (Fig. 7). All these lipid classes presented an increase in peak height between 2 and 6 times and an increase in peak area between 2 and 8 times (Table 2).

Third, in addition to the decreased retention time described for PAs before, PIs, PSs, and PGs also presented a decrease in retention when using 2.5 mM ABC buffers (Table S3). In contrast, major lipids such as PCs and PEs did not show a significant change in retention. Thus, using ABC improves the resolution between major and minor lipids, decreasing the risk of interferences and ion suppression of minor lipids.

Beyond these effects, ABC buffers give an extra advantage for the structural determination of the lipids with a choline moiety (LPCs, PCs and SMs).

LPCs, PCs and SMs all have a quaternary ammonium function in their

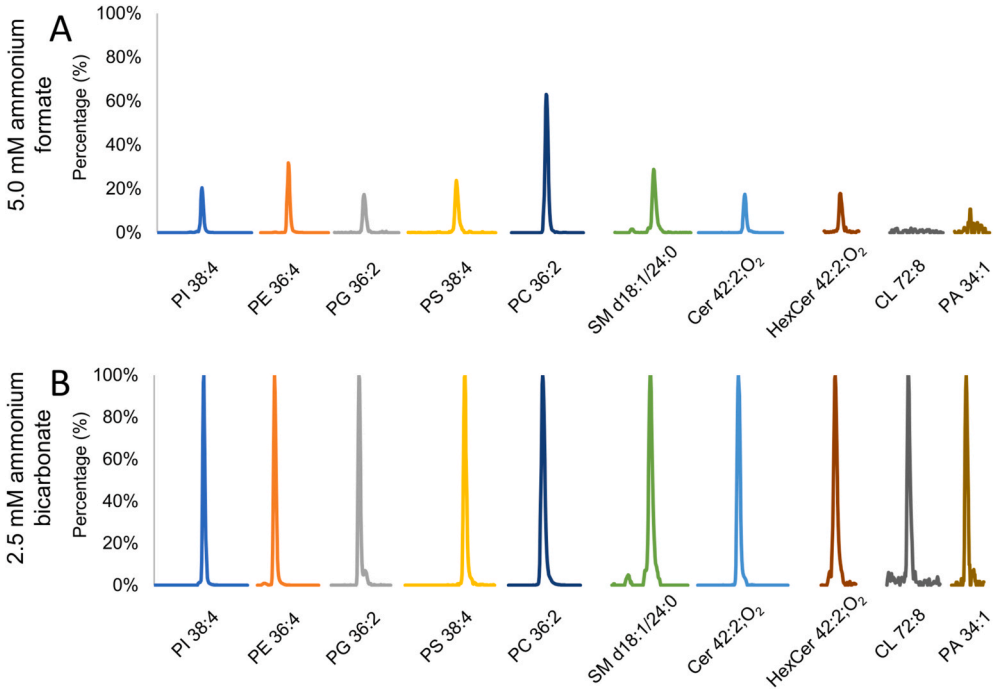

Fig. 7. Effect of ammonium formate and ammonium bicarbonate buffers on the peak height of different lipid species in liver samples. Extracted ion chromatograms in negative mode, comparison in relative intensity for specific phospholipids and sphingolipids species using an HST-CSH C18 column between the buffers: (A) 5.0 mM ammonium formate (AFO); and (B) 2.5 mM ammonium bicarbonate (ABC). Y-axis shows the relative intensity for each EIC (normalized to 100 % when the lipid was analyzed with 2.5 mM ABC). X-axis is not in retention order.

Table 2
Effect of ammonium bicarbonate buffers on the peak height and the peak area of different lipid classes in liver samples. Fold change of the peak height and area when using 2.5 mM ABC buffer in comparison with 5.0 mM AFO buffer. The mean and the standard deviation (st.dev) were calculated across the lipid species in each family (Table S3). LPS and CL are non-applicable (n.a.) since they were non-detectable with the AFO buffer.

HST-CSH c18 column	Peak Height		Peak Area	
	mean	st.dev.	mean	st.dev.
LPA	28	10	34	17
HexCer	6.0	0.4	8.1	1.3
PI	5.6	1.8	5.0	2.5
Cer	4.8	1.4	4.9	1.4
PS	4.5	1.5	4.3	1.6
PG	4.0	1.4	3.8	1.5
PE	3.7	1.4	3.5	1.5
LPE	3.0	0.7	2.9	0.6
SM	2.8	0.8	2.9	0.9
PC	2.2	0.8	2.4	0.8
LPC	1.4	0.1	1.4	0.1
LPS	n.a.	n.a.	n.a.	n.a.
CL	n.a.	n.a.	n.a.	n.a.

polar headgroup, which easily forms adducts in negative mode by its association with anions in the buffer. The adduct $[M + HCO3]^-$ for especially PCs, presents the advantage of facilitating the determination of regioisomers through structural elucidation of the sn-1 and sn-2 position of the fatty acyl chains of PCs and SMs [26–28]. A specific MS/MS fragmentation facilitates the qualitative determination for the two classes of lipids and their isomers which are crucial for the understanding of the lipidome and its connection to different diseases or therapies.

In summary, our results show that 2.5 mM ABC buffers improve the detectability of the lipidome (PLs and sphingolipids) in biological samples by three factors: (i) increased peak symmetry for strongly tailing lipids; (ii) enhanced ionization in ESI; and (iii) increased separation between major and minor lipids. This increase in detectability is of special importance for PAs and CLs, whose detection was not possible with traditional AFO on C18 reversed phase columns.

4. Conclusions

Our work has improved the coverage of the lipidome in reversed phase chromatography and negative ESI-MS detection. ABC buffers for RPLC separation of lipids improved the chromatographic peak symmetry of strongly tailing lipids (PA, PS, CL, CerP, PI-P, PI-P2, S–1P) and enhanced the detectability of all studied lipids. We found small drifts in retention time and mass spectrometry signals. However, these effects were similar to those of other common buffers and could be corrected by using quality control samples as is customary in lipidomics. Despite this drift we could still detect the lipids at a higher S/N ratio with ABC than AFO.

Using lower concentration of ABC increased the ionization efficiency in the ion source as well resulting in higher chromatographic resolution between low and high abundant lipids. Consequently, moving from traditional AFO buffers to new ABC buffers, RPLC will allow a broader coverage of the aforementioned chromatographically problematic lipids together with other phospholipids in a single run. This expansion will boost the lipidomics analytical productivity and yield an improved biological information regarding metabolism and cell signaling. This is especially important for PAs and CLs, which are fundamental for the synthesis of other phospholipids and for mitochondrial function [44,45]. Consequently, beyond the general improvement in the analysis of the lipidome, we expect specifically that the implementation of our method will improve future investigations of the role of cardiolipins in different physiological and pathophysiological processes, such as ferroptosis and Barth syndrome [44,46].

CRediT authorship contribution statement

Jenny M. Nilsson: Writing – review & editing, Writing – original draft, Methodology, Investigation, Formal analysis, Conceptualization. **David Balgoma:** Writing – review & editing, Supervision, Methodology, Investigation, Conceptualization. **Curt Pettersson:** Writing – review & editing, Supervision. **Hans Lennernäs:** Writing – review & editing. **Femke Heindryckx:** Writing – review & editing, Funding acquisition. **Mikael Hedeland:** Writing – review & editing, Supervision, Project administration, Methodology, Funding acquisition, Conceptualization.

Declaration of competing interest

There is no conflict of interest from the authors of this article.

Data availability

Data will be made available on request.

Acknowledgments

M.H. acknowledges support from the Swedish Research Council (grant no 2023-04500).

D.B. acknowledges support from María Zambrano Fellowship (Next Generation EU), Proyecto de Internacionalización de la Unidad de Excelencia IBGM (CL-EI-2021 IBGM) and Programa Estratégico IBGM (CCVC8485).

F.H. acknowledges support from Cancerfonden (grant no. 232776 Pj).

Appendix A. Supplementary data

Supplementary data to this article can be found online at https://doi.org/10.1016/j.aca.2024.342811.

References

[1] S.-C. Kim, X. Wang, Phosphatidic acid: an emerging versatile class of cellular mediators, Essays Biochem. 64 (3) (Sep. 2020) 533–546, https://doi.org/10.1042/EBC20190089.
[2] O. Quehenberger, et al., Lipidomics reveals a remarkable diversity of lipids in human plasma, J. Lipid Res. 51 (11) (Nov. 2010) 3299–3305, https://doi.org/10.1194/jlr.M009449.
[3] Y. Liu, Y. Su, X. Wang, Phosphatidic acid-mediated signaling, in: D.G.S. Capelluto (Ed.), Lipid-mediated Protein Signaling, vol. 991, Springer Netherlands, Dordrecht, 2013, pp. 159–176, https://doi.org/10.1007/978-94-007-6331-9_9. Advances in Experimental Medicine and Biology, vol. 991.
[4] D. Balgoma, A. Checa, D.G. Sar, S. Snowden, C.E. Wheelock, Quantitative metabolic profiling of lipid mediators, Mol. Nutr. Food Res. 57 (8) (Aug. 2013) 1359–1377, https://doi.org/10.1002/mnfr.201200840.
[5] F. Sakane, F. Hoshino, C. Murakami, New Era of diacylglycerol kinase, phosphatidic acid and phosphatidic acid-binding protein, Int. J. Mol. Sci. 21 (18) (Sep. 2020) 6794, https://doi.org/10.3390/ijms21186794.
[6] G. Van Meer, D.R. Voelker, G.W. Feigenson, Membrane lipids: where they are and how they behave, Nat. Rev. Mol. Cell Biol. 9 (2) (Feb. 2008) 112–124, https://doi.org/10.1038/nrm2330.
[7] D. English, Y. Cui, R.A. Siddiqui, Messenger functions of phosphatidic acid, Chem. Phys. Lipids 80 (1–2) (May 1996) 117–132, https://doi.org/10.1016/0009-3084(96)02549-2.
[8] J. Zegarlinska, M. Piaścik, A.F. Sikorski, A. Czogalla, Phosphatidic acid – a simple phospholipid with multiple faces, Acta Biochim. Pol. 65 (2) (Jul. 2018) 163–171, https://doi.org/10.18388/abp.2018_2592.
[9] H. Ogiso, T. Suzuki, R. Taguchi, Development of a reverse-phase liquid chromatography electrospray ionization mass spectrometry method for lipidomics, improving detection of phosphatidic acid and phosphatidylserine, Anal. Biochem. 375 (1) (Apr. 2008) 124–131, https://doi.org/10.1016/j.ab.2007.12.027.
[10] G. Isaac, I.D. Wilson, R.S. Plumb, Application of hybrid surface technology for improving sensitivity and peak shape of phosphorylated lipids such as phosphatidic acid and phosphatidylserine, J. Chromatogr. A 1669 (Apr. 2022) 462921, https://doi.org/10.1016/j.chroma.2022.462921.
[11] T. Cajka, O. Fiehn, Increasing lipidomic coverage by selecting optimal mobile-phase modifiers in LC–MS of blood plasma, Metabolomics 12 (2) (Feb. 2016) 34, https://doi.org/10.1007/s11306-015-0929-x.
[12] Y. Sato, T. Nakamura, K. Aoshima, Y. Oda, Quantitative and wide-ranging profiling of phospholipids in human plasma by two-dimensional liquid chromatography/

mass spectrometry, Anal. Chem. 82 (23) (Dec. 2010) 9858–9864, https://doi.org/10.1021/ac102211r.
[13] J. Zhang, Q. Wang, B. Kleintop, T. Raglione, Suppression of peak tailing of phosphate prodrugs in reversed-phase liquid chromatography, J. Pharm. Biomed. Anal. 98 (Sep. 2014) 247–252, https://doi.org/10.1016/j.jpba.2014.05.027.
[14] A. Wakamatsu, K. Morimoto, M. Shimizu, S. Kudoh, A severe peak tailing of phosphate compounds caused by interaction with stainless steel used for liquid chromatography and electrospray mass spectrometry, J. Separ. Sci. 28 (14) (Sep. 2005) 1823–1830, https://doi.org/10.1002/jssc.200400027.
[15] Y. Asakawa, N. Tokida, C. Ozawa, M. Ishiba, O. Tagaya, N. Asakawa, Suppression effects of carbonate on the interaction between stainless steel and phosphate groups of phosphate compounds in high-performance liquid chromatography and electrospray ionization mass spectrometry, J. Chromatogr. A 1198 (1199) (Jul. 2008) 80–86, https://doi.org/10.1016/j.chroma.2008.05.015.
[16] R. Tuytten, et al., Stainless steel electrospray probe: a dead end for phosphorylated organic compounds? J. Chromatogr. A 1104 (1–2) (Feb. 2006) 209–221, https://doi.org/10.1016/j.chroma.2005.12.004.
[17] O.L. Knittelfelder, B.P. Weberhofer, T.O. Eichmann, S.D. Kohlwein, G. N. Rechberger, A versatile ultra-high performance LC-MS method for lipid profiling, J. Chromatogr. B 951–952 (Mar. 2014) 119–128, https://doi.org/10.1016/j.jchromb.2014.01.011.
[18] J.L. Spalding, F.J. Naser, N.G. Mahieu, S.L. Johnson, G.J. Patti, Trace phosphate improves ZIC-pHilic peak shape, sensitivity, and coverage for untargeted metabolomics, J. Proteome Res. 17 (10) (Oct. 2018) 3537–3546, https://doi.org/10.1021/acs.jproteome.8b00487.
[19] K.T. Myint, T. Uehara, K. Aoshima, Y. Oda, Polar anionic metabolome analysis by nano-LC/MS with a metal chelating agent, Anal. Chem. 81 (18) (Sep. 2009) 7766–7772, https://doi.org/10.1021/ac901269h.
[20] M. DeLano, et al., Using hybrid organic–inorganic surface technology to mitigate analyte interactions with metal surfaces in UHPLC, Anal. Chem. 93 (14) (Apr. 2021) 5773–5781, https://doi.org/10.1021/acs.analchem.0c05203.
[21] N. Tanna, L.G. Mullin, P.D. Rainville, I.D. Wilson, R.S. Plumb, Improving LC/MS/MS-based bioanalytical method performance and sensitivity via a hybrid surface barrier to mitigate analyte – metal surface interactions, J. Chromatogr. B 1179 (Aug. 2021) 122825, https://doi.org/10.1016/j.jchromb.2021.122825.
[22] K.D. Wyndham, et al., Characterization and evaluation of C $_{18}$ HPLC stationary phases based on ethyl-bridged hybrid organic/inorganic particles, Anal. Chem. 75 (24) (Dec. 2003) 6781–6788, https://doi.org/10.1021/ac034767w.
[23] D.S. Gertner, D.P. Bishop, M.P. Padula, Optimization of chromatographic buffer conditions for the simultaneous analysis of phosphatidylinositol and phosphatidylinositol phosphate species in canola, J. Separ. Sci. (Jun. 2023) 2300165, https://doi.org/10.1002/jssc.202300165.
[24] R. Yin, S. Liu, C. Zhao, M. Lu, M. Tang, H. Wang, An ammonium bicarbonate-enhanced stable isotope dilution UHPLC-MS/MS method for sensitive and accurate quantification of acrolein–DNA adducts in human leukocytes, Anal. Chem. 85 (6) (Mar. 2013) 3190–3197, https://doi.org/10.1021/ac3034695.
[25] M. Pulfer, R.C. Murphy, Electrospray mass spectrometry of phospholipids, Mass Spectrom. Rev. 22 (5) (Sep. 2003) 332–364, https://doi.org/10.1002/mas.10061.
[26] X. Zhao, G. Wu, W. Zhang, M. Dong, Y. Xia, Resolving modifications on sphingoid base and *N* -acyl chain of sphingomyelin lipids in complex lipid extracts, Anal. Chem. 92 (21) (Nov. 2020) 14775–14782, https://doi.org/10.1021/acs.analchem.0c03502.
[27] X. Zhao, et al., A lipidomic workflow capable of resolving *sn* - and C C location isomers of phosphatidylcholines, Chem. Sci. 10 (46) (2019) 10740–10748, https://doi.org/10.1039/C9SC03521D.
[28] X. Zhao, Y. Xia, Characterization of fatty acyl modifications in phosphatidylcholines and lysophosphatidylcholines via radical-directed dissociation, J. Am. Soc. Mass Spectrom. 32 (2) (Feb. 2021) 560–568, https://doi.org/10.1021/jasms.0c00407.
[29] D. Balgoma, et al., Orthogonality in principal component analysis allows the discovery of lipids in the jejunum that are independent of ad libitum feeding, Metabolites 12 (9) (Sep. 2022) 866, https://doi.org/10.3390/metabo12090866.
[30] E.G. Bligh, W.J. Dyer, A rapid method of total lipid extraction and purification, Can. J. Biochem. Physiol. 37 (8) (Aug. 1959) 911–917, https://doi.org/10.1139/o59-099.
[31] S. Nakagawa, I.C. Cuthill, Effect size, confidence interval and statistical significance: a practical guide for biologists, Biol. Rev. 82 (4) (Nov. 2007) 591–605, https://doi.org/10.1111/j.1469-185X.2007.00027.x.
[32] O. Montero, M. Hedeland, D. Balgoma, Trials and tribulations of statistical significance in biochemistry and omics, Trends Biochem. Sci. 48 (6) (Jun. 2023) 503–512, https://doi.org/10.1016/j.tibs.2023.01.009.
[33] G. Liebisch, et al., Update on LIPID MAPS classification, nomenclature, and shorthand notation for MS-derived lipid structures, J. Lipid Res. 61 (12) (Dec. 2020) 1539–1555, https://doi.org/10.1194/jlr.S120001025.
[34] D. Balgoma, S. Zelleroth, A. Grönbladh, M. Hallberg, C. Pettersson, M. Hedeland, Anabolic androgenic steroids exert a selective remodeling of the plasma lipidome that mirrors the decrease of the de novo lipogenesis in the liver, Metabolomics 16 (1) (Jan. 2020) 12, https://doi.org/10.1007/s11306-019-1632-0.
[35] D. Balgoma, et al., Anthracyclins increase PUFAs: potential implications in ER stress and cell death, Cells 10 (5) (May 2021) 1163, https://doi.org/10.3390/cells10051163.
[36] K.-H. Huang, Z. Wei, R.G. Cooks, Accelerated reactions of amines with carbon dioxide driven by superacid at the microdroplet interface, Chem. Sci. 12 (6) (2021) 2242–2250, https://doi.org/10.1039/D0SC05625A.
[37] L. Feng, et al., Ammonium bicarbonate significantly accelerates the microdroplet reactions of amines with carbon dioxide, Anal. Chem. 93 (47) (Nov. 2021) 15775–15784, https://doi.org/10.1021/acs.analchem.1c03954.
[38] M. Girod, E. Moyano, D.I. Campbell, R.G. Cooks, Accelerated bimolecular reactions in microdroplets studied by desorption electrospray ionization mass spectrometry, Chem. Sci. 2 (3) (2011) 501–510, https://doi.org/10.1039/C0SC00416B.
[39] S. Abreu, A. Solgadi, P. Chaminade, Optimization of normal phase chromatographic conditions for lipid analysis and comparison of associated detection techniques, J. Chromatogr. A 1514 (Sep. 2017) 54–71, https://doi.org/10.1016/j.chroma.2017.07.063.
[40] A. Castellaneta, et al., HILIC-ESI-MS analysis of phosphatidic acid methyl esters artificially generated during lipid extraction from microgreen crops, J. Mass Spectrom. 56 (10) (Oct. 2021), https://doi.org/10.1002/jms.4784.
[41] L. Gao, S. Ji, B. Burla, M.R. Wenk, F. Torta, A. Cazenave-Gassiot, LICAR: an application for isotopic correction of targeted lipidomic data acquired with class-based chromatographic separations using multiple reaction monitoring, Anal. Chem. 93 (6) (Feb. 2021) 3163–3171, https://doi.org/10.1021/acs.analchem.0c04565.
[42] E. Cífková, R. Hájek, M. Lísa, M. HolŁapek, Hydrophilic interaction liquid chromatography mass spectrometry of (lyso)phosphatidic acids, (lyso) phosphatidylserines and other lipid classes, J. Chromatogr. A 1439 (Mar. 2016) 65–73, https://doi.org/10.1016/j.chroma.2016.01.064.
[43] O. Peterka, et al., HILIC/MS quantitation of low-abundant phospholipids and sphingolipids in human plasma and serum: dysregulation in pancreatic cancer, Anal. Chim. Acta 1288 (Feb. 2024) 342144, https://doi.org/10.1016/j.aca.2023.342144.
[44] H. Yuan, X. Li, X. Zhang, R. Kang, D. Tang, CISD1 inhibits ferroptosis by protection against mitochondrial lipid peroxidation, Biochem. Biophys. Res. Commun. 478 (2) (Sep. 2016) 838–844, https://doi.org/10.1016/j.bbrc.2016.08.034.
[45] S.T. Ahmadpour, K. Mahéo, S. Servais, L. Brisson, J.-F. Dumas, Cardiolipin, the mitochondrial signature lipid: implication in cancer, Int. J. Mol. Sci. 21 (21) (Oct. 2020) 8031, https://doi.org/10.3390/ijms21218031.
[46] A.J. Chicco, G.C. Sparagna, Role of cardiolipin alterations in mitochondrial dysfunction and disease, Am. J. Physiol. Cell Physiol. 292 (1) (Jan. 2007) C33–C44, https://doi.org/10.1152/ajpcell.00243.2006.